

# Magnetic moments of Ni monolayers and small ground-state Ni clusters at the Al (001) surface

R. Robles

*Departamento de Física Teórica, Atómica, Molecular y Nuclear, Universidad de Valladolid, E-47011 Valladolid, Spain*

R. C. Longo

*Departamento de Física de la Materia Condensada, Facultad de Física, Universidad de Santiago de Compostela, E-15706 Santiago de Compostela, Spain*

A. Vega

*Departamento de Física Teórica, Atómica, Molecular y Nuclear, Universidad de Valladolid, E-47011 Valladolid, Spain*

L. J. Gallego

*Departamento de Física de la Materia Condensada, Facultad de Física, Universidad de Santiago de Compostela, E-15706 Santiago de Compostela, Spain*

(Received 13 December 1999)

Using the embedded atom model potential proposed for Ni-Al systems by Voter and Chen, we performed molecular-dynamics simulations to compute the quenched structures of small  $Ni_n$  clusters ( $n \leq 10$ ) deposited on or just beneath the Al (001) surface. Embedded clusters were always more stable than adsorbed clusters. Determination of spin-polarized electronic structures using a self-consistent *spd* tight-binding method showed that, due to hybridization between the Al *sp* and Ni *d* states, embedded  $Ni_n$  clusters and adsorbed or embedded Ni monolayers are nonmagnetic.

## I. INTRODUCTION

Over the last few years, the interaction of thin films of transition metals with Al surfaces has attracted considerable attention because of the potential technological applications of transition-metal aluminides as light-weight heat-resistant structural materials<sup>1</sup> and as metalization layers on semiconductors.<sup>2</sup> Most of the work in this area has been experimental. In particular, Shutthanandan and co-workers<sup>3-9</sup> have used high-energy ion scattering, x-ray photoemission spectroscopy and low-energy electron diffraction to study the growth modes and interface structures of ultrathin Ni, Pd, Fe, and Ti films deposited on single crystal Al surfaces at room temperature. They reported that Ti grew as an epitaxial overlayer on both (110) and (001) surfaces, that Pd and Fe always formed surface alloys with the substrate, and that Ni formed an alloy at the (110) surface but tended to form an overlayer on the (001) surface. Their experimental results for Ni/Al(110) (Ref. 3) were subsequently<sup>4</sup> reproduced in Monte Carlo simulations using the embedded atom model (EAM) potential that had been proposed for Ni-Al alloys by Voter and Chen (VC).<sup>10</sup> This potential has recently been used by Longo *et al.*<sup>11</sup> in quenched molecular dynamics (MD) simulations to compute the structures and binding energies of small Ni clusters and a full Ni monolayer on the Al (001) surface. Longo *et al.*'s results suggested that both the clusters and the monolayer undergo surface alloying, but whereas the surface alloying of the clusters occurs rapidly, that of the monolayer requires an appreciable prior equilibration period at a temperature allowing atomic mobility; quenching without this equilibration period can freeze the system in a state in which the adsorbed Ni layer remains on an Al surface that is hardly altered. This latter finding sug-

gests that the Ni films constructed on the Al (001) surface by Shutthanandan *et al.*<sup>6</sup> were probably metastable.

The cluster calculations performed by Longo *et al.*<sup>11</sup> were intended only to determine whether Ni atoms deposited on the surface tended to be embedded in the Al substrate, displacing Al atoms from their initial positions, or remained on top of the slab at fourfold adsorption sites. No attempt was made to compute the ground-state structures of the clusters. The aim of the paper described here was twofold. First, we wished to determine the ground-state configurations of small Ni clusters at the Al (001) surface, within the VC EAM, by quenching clusters placed in numerous starting configurations both on and beneath the surface. Second, we wanted to determine the magnetic properties of the ground-state clusters, which are not calculable using the EAM, in order to see whether or not their magnetic moments are "deadened" by the nonmagnetic Al surface. In view of the numbers of non-equivalent sites in these systems, for this latter purpose we used a self-consistent tight-binding (TB) model similar to that used by Izquierdo *et al.*<sup>12</sup> to analyze the magnetism of Co nanoparticles supported on the Cu (111) surface. Determination of both geometries and magnetic moments with the TB model was deemed unfeasible for the systems considered in this paper because of the great computational effort that would be involved in performing self-consistent electronic calculations at each step of the geometric optimization (in cluster physics, self-consistent calculations of both geometry and electronic structure are generally limited to small free clusters; see, e.g., Ref. 13).

The validity of the strategy of first using an *n*-body potential to determine ground-state structures and a TB model to obtain their magnetic moments, which has a precedent in Bouarab *et al.*'s<sup>14</sup> successful calculation of the observed<sup>15</sup>

average magnetic moments of free-standing  $Ni_n$  clusters using the so-called Gupta-like potential<sup>16</sup> for the structural description, depends on the accuracy of the ground-state geometry located in the first stage. The reliability of the structural calculations performed in this paper is supported by the past success of EAM potentials in describing the structures of metal-atom clusters supported on metal surfaces. For instance, results obtained by Schwoebel *et al.*<sup>17</sup> for Pt clusters on Pt(001) using the EAM method of Foiles *et al.*<sup>18</sup> (FBD) agree with the results of field-ion microscopy (FIM) in predicting that clusters oscillate between chain and island-type configurations as the number of adatoms increases from three to six; and Fallis *et al.*'s<sup>19</sup> predictions for the most stable structures of small Pt clusters on Pt(111) using the VC EAM agree, with few exceptions, with the geometries observed in FIM studies of Ir clusters on Ir(111).<sup>20</sup> Hence it is reasonable to assume that the behavior of  $Ni_n$  clusters on Al(001) is well described by the VC EAM Ni-Al potential,<sup>10</sup> in spite of its being largely (but not entirely) parametrized on the basis of bulk properties (see below). It is worth pointing out that the structural features of small free Ni-Al clusters predicted using the VC EAM Ni-Al potential<sup>21</sup> agree with the results afforded by a self-consistent density-functional method.<sup>22</sup>

As regards the electronic calculations, the self-consistent TB method is known to be capable of correct description of the electronic structures and itinerant magnetism of a great variety of transition-metal systems, including free-standing clusters,<sup>14</sup> supported clusters,<sup>12</sup> and surfaces and multilayers.<sup>23</sup> Moreover, as is reported below, for Ni monolayers on or just below the Al (001) surface, this method affords results similar to those obtained using the *ab initio* tight-binding linear muffin-tin orbital method (TB-LMTO) with the atomic sphere approximation.<sup>24,25</sup>

Details of the computations performed to determine the ground-state structures of  $Ni_n$  clusters up to  $n = 10$  at the Al (001) surface, and of the method used to compute their magnetic moments, are given in Sec. II. In Sec. III we present and discuss our results, and in Sec. IV we summarize our main conclusions.

## II. COMPUTATIONAL PROCEDURE AND THEORETICAL BACKGROUND

As indicated above, we computed the ground-state structures of small Ni clusters on the Al (001) surface using the VC version of the EAM, which has an embedding function and pair interaction parametrized using properties of the diatomic molecule as well as bulk properties. In particular, the parameters of the Ni-Al potential were optimized by Voter and Chen<sup>10</sup> so as to fit the model to the following large set of experimental data: the elastic constants and vacancy formation energies of pure fcc Ni and pure fcc Al, the bond lengths and bond energies of the diatomic molecules  $Ni_2$  and  $Al_2$ , the lattice constant, cohesive energy, elastic constants, vacancy formation energy, antiphase boundary energies, and superintrinsic stacking fault energy of  $Ni_3Al$  ( $L1_2$ ), and the lattice constant and cohesive energy of the  $B2$  phase NiAl. It is Voter and Chen's values that were used to calculate, during our simulations, the forces experienced by the atoms in the  $Ni_n/Al(001)$  systems.

The Al (001) surface was modeled by the top (001) layer of a 15-layer slab of atoms with the bottom 4 layers fixed and periodic boundary conditions along the [100] and [010] directions. Each layer is comprised of 450-Al atoms. The atoms in the slab were initially arranged as in bulk Al, but before addition of the Ni atoms the top 11 layers were relaxed to the minimum-energy configuration using a conjugated gradient procedure.<sup>26</sup> As in Ref. 11, we computed the lowest-energy structures of  $Ni_n$  clusters at the surface by choosing various initial configurations for each value of  $n$  and, for each configuration, calculating the minimum energy of the cluster+substrate system using a quenched MD minimization technique in which the velocity of an atom is set to zero whenever the scalar product of its velocity and acceleration becomes negative.<sup>27</sup> The main difference with respect to the analysis performed in Ref. 11 was that we now included, among the starting configurations, configurations in which the  $Ni_n$  clusters were below the Al (001) surface, i.e., were substitutional impurities embedded in the substrate rather than adsorbed clusters. The set of embedded starting configurations included states with clusters of various shapes embedded in a single one of the top few layers, and states with clusters occupying various layers. In all cases, the initial positions of the displaced Al atoms were above top-layer fourfold symmetry sites lying over the embedded clusters.

Using the cluster geometries and interatomic distances obtained as described above, we computed the magnetic-moments distribution of the  $Ni_n/Al(001)$  systems as follows. The spin-polarized electronic structure of the deposited Ni clusters and their surrounding Al atoms was determined by self-consistently solving a TB Hamiltonian for the  $s$ ,  $p$ , and  $d$  valence electrons in a mean-field approximation.<sup>12,28</sup> In the usual second quantization notation, the real-space Hamiltonian  $H$  is given by

$$H = \sum_{i,\alpha,\sigma} \epsilon_{i\alpha\sigma} N_{i\alpha\sigma} + \sum_{\substack{i,\alpha,\sigma \\ i \neq j}} t_{ij}^{\alpha\beta} c_{i\alpha\sigma}^\dagger c_{j\beta\sigma}, \quad (1)$$

where  $c_{i\alpha\sigma}^\dagger$  ( $c_{j\beta\sigma}$ ) is the operator for the creation (annihilation) of an electron with spin  $\sigma$  and orbital state  $\alpha$  ( $\beta$ ) at atomic site  $i$  ( $j$ ), and  $N_{i\alpha\sigma}$  is the number operator. Electron delocalization within the system is described by the hopping integrals  $t_{ij}^{\alpha\beta}$ , which we included up to the second neighbors and assumed to be spin independent. The hopping integrals between atoms of the same element were determined using the Slater-Koster approximation, with two-center hopping integrals reproducing the band structure of the bulk metal taken from Papaconstantopoulos' *Handbook of the Band Structure of Elemental Solids*.<sup>29</sup> Since the interatomic distances given by the MD simulations differed a little from the distances in the bulk, we assumed that in the neighborhood of the ideal first- and second-nearest neighbor distances the hopping integrals obey the usual power law  $(r_0/r_{ij})^{l+l'+1}$ , where  $r_0$  is the bulk first- (or second-) nearest-neighbor distance, and  $l$  and  $l'$  are the orbital angular momenta of the spin-orbital states involved in the hopping process.<sup>30</sup> The heteronuclear hoppings were calculated as the average of the corresponding homonuclear hoppings.

The spin-dependent diagonal terms  $\epsilon_{i\alpha\sigma}$  in the Hamiltonian include electron-electron interaction through a correction of the energy levels, and are given by

$$\epsilon_{i\alpha\sigma} = \epsilon_{i\alpha}^0 + z_\sigma \sum_\beta \frac{J_{i,\alpha\beta}}{2} \mu_{i\beta} + \Omega_{i\alpha}. \quad (2)$$

Here,  $\epsilon_{i\alpha}^0$  is the bare energy of orbital  $\alpha$  at site  $i$  (that is, excluding Coulomb interactions). The second term is the correction for spin polarization of the electrons at site  $i$  ( $\mu_{i\beta} = \langle N_{i\beta\uparrow} \rangle - \langle N_{i\beta\downarrow} \rangle$ ), that is, the local magnetic moment excluding the orbital part. In this second term, the  $J_{i,\alpha\beta}$  are the exchange integrals and  $z_\sigma$  is the sign function ( $z_\uparrow = +1$ ;  $z_\downarrow = -1$ ). As usual, we neglected the exchange integrals involving  $sp$  electrons, taking into account only the integral corresponding to the  $d$  electrons of Ni. (Note that spin polarization of the delocalized  $sp$  band is also possible as a consequence of hybridization with the  $d$  states.)  $J = J_{dd}(\text{Ni})$  was optimized so as to reproduce the local magnetic moments of bulk fcc Ni, of an Ni monolayer supported on the Al (001) surface, and of Ni monolayers embedded one and two layers below that surface, the interlayer distances being determined using the same geometrical optimization procedure as for the deposited clusters; the local magnetic moment values to be reproduced were obtained using a  $k$ -space scalar relativistic version of the *ab initio* TB-LMTO method with the atomic sphere approximation<sup>24,25</sup> (this method is based on the local spin-density approximation<sup>31</sup> of the density-functional theory<sup>32,33</sup>). Finally, the site and orbital-dependent potentials  $\Omega_{i\alpha}$  were self-consistently determined in order to obtain the *ab initio*  $sp$  and  $d$  occupations of an ideal Ni monolayer embedded two layers below the Al (001) surface.

The magnetic-moments distribution was determined by integrating the majority and minority local densities-of-states (LDOS) up to the Fermi energy. The LDOS were obtained from the diagonal elements of the Green function, which were computed using the recursion method<sup>34</sup> with a sufficient number of levels in the continued fraction to ensure the stability of the results.

### III. RESULTS AND DISCUSSION

Our VC EAM structural calculations for  $\text{Ni}_n/\text{Al}(001)$  systems showed that, for each  $n$ , the most stable configuration was an embedded structure obtained by quenching an embedded starting configuration. In particular, these lowest-energy embedded structures were in all cases more stable than the most stable structure obtained by quenching an adsorbed starting configuration (Table I). Similar results have been found by Patthey *et al.*<sup>35</sup> and Schneider *et al.*<sup>36</sup> for Pd clusters on Ag(001) and Ag(110), respectively, using the FBD version of the EAM.<sup>18</sup> As Fig. 1 shows, the lowest-energy Ni clusters were generally close-packed islands embedded in the second layer of the Al substrate; the only exception was  $\text{Ni}_2$ , which was embedded in the third layer, although this configuration is almost isoenergetic with another in which the two Ni atoms are embedded in the second layer. Hence our results confirm the tendency for Ni atoms to be embedded in the Al (001) surface that was observed in Ref. 11. We assume that clusters deposited on the surface at room temperature (say) would eventually adopt the lowest-

TABLE I. Comparison of the minimum energies of  $\text{Ni}_n/\text{Al}(001)$  systems ( $n=2-10$ ) for adsorbed clusters (structures reported in Ref. 11) and embedded clusters (structures shown in Fig. 1), as obtained using the VC EAM Ni-Al potential. Units are in eV.

| $n$ | Adsorbed    | Embedded    |
|-----|-------------|-------------|
| 2   | -22293.5870 | -22294.6783 |
| 3   | -22298.4158 | -22299.8689 |
| 4   | -22302.7250 | -22305.2620 |
| 5   | -22307.7903 | -22310.3024 |
| 6   | -22312.5997 | -22315.6355 |
| 7   | -22317.1463 | -22320.8124 |
| 8   | -22321.7012 | -22326.0788 |
| 9   | -22326.4605 | -22331.3352 |
| 10  | -22331.2144 | -22336.5586 |

energy embedded structures if annealed slowly enough.

The TB-LMTO results for the electronic structures of Ni monolayers supported on Al(001) or embedded below the surface show that the Ni atoms lose their magnetic moments due to hybridization with the  $sp$  states of Al. Note that when the Ni monolayer is deposited on the Al surface, Ni-Ni distances are longer than in pure fcc Ni because the lattice parameter of Al (4.05 Å) is larger than that of Ni (3.52 Å),<sup>37</sup> and that in the absence of Ni-Al hybridization the magnetic moments of the Ni atoms would therefore be larger than in the bulk, being closer to the atomic limit.

The hybridization is reflected in the LDOS, shown in Fig. 2 for some inequivalent sites of a system composed of an Ni monolayer embedded two layers below the Al (001) surface [the results for the Ni monolayer resting on top of Al(001) and for the Ni monolayer embedded one layer below the surface exhibit similar characteristics, and for the sake of brevity are not shown here]. In this case, the inequivalent sites represent different (001) layers. Below the Fermi level,

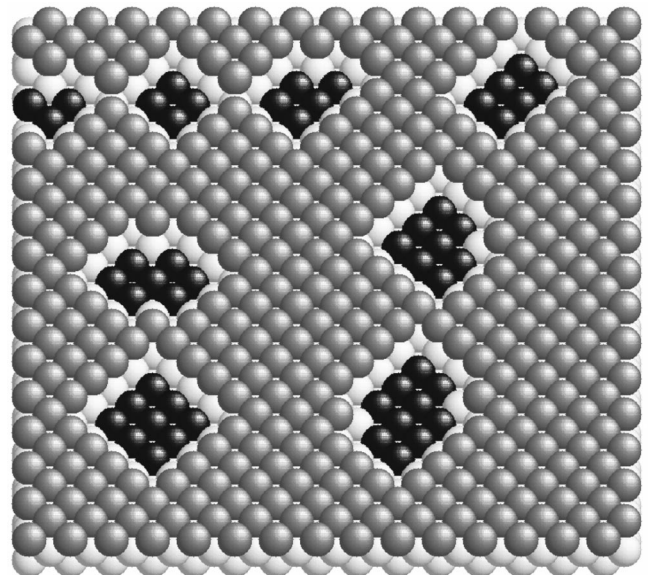


FIG. 1. Predicted ground-state structures of  $\text{Ni}_n$  clusters at the Al (001) surface (dark spheres represent Ni atoms; for clarity, the Al atoms situated above the Ni clusters have been removed).



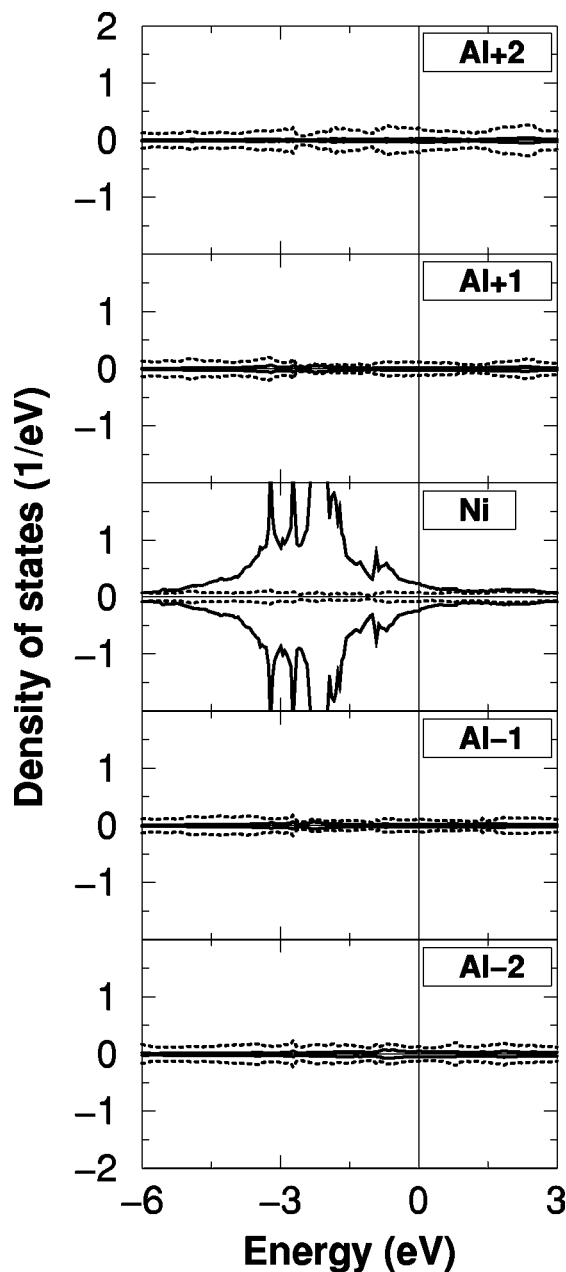


FIG. 2. Local densities of electronic states (LDOS) at some inequivalent sites [different (001) layers] of the system formed by an Ni monolayer embedded two layers below the Al (001) surface, as calculated using the *ab initio* TB-LMTO method. The LDOS at the Al sites located  $n$  layers above or below the Ni layer are labeled Al+ $n$  or Al- $n$ , respectively (Al+2 corresponds, therefore, to the Al surface layer). The  $d$  projection of the LDOS is plotted with a solid line, the  $sp$  projection with a dotted line. The upper (lower) part of the LDOS corresponds to the spin-up (spin-down) projection. The vertical line indicates the Fermi level.

the Ni LDOS is composed of localized  $d$ -type states with negligible  $sp$  character, and of delocalized  $sp$ -type states reflecting  $sp$ - $d$  hybridization mainly at the borders of the  $d$ -type band, where the electronic states have similar degrees of  $d$  and  $sp$  character. As a consequence of the  $sp$ - $d$  hybridization, the effective  $d$  bandwidth increases (notice that strong  $d$  character persists up to at least 3 eV above the Fermi level).

In a study of free-standing Fe clusters using a TB model

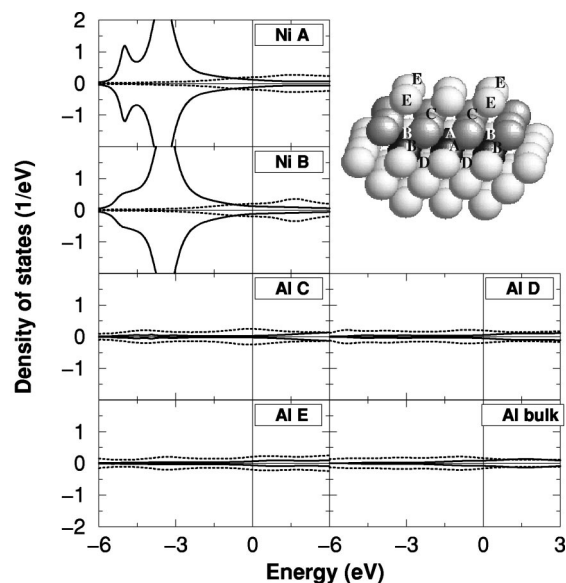


FIG. 3. Local densities of electronic states (LDOS) at some representative inequivalent sites of the  $Ni_6/Al(001)$  system, as calculated using the self-consistent TB model (only a portion of the model system is shown): Ni A, central Ni atoms; Ni B, Ni atoms at the cluster ends; Al C, top-layer Al atoms resting on four Ni atoms; Al D, third-layer Al atoms under four Ni atoms; Al E, displaced Al atoms on top of the top layer and laying over Ni B atoms. Orbital and spin projections are plotted as in Fig. 2. The lower resolution of this plot as compared with that of Fig. 2 is a consequence of the Lorentzian broadening in the recursion method used in the TB calculations.

similar to that employed here, Vega *et al.*<sup>28</sup> found that  $sp$ - $d$  hybridization tended to reduce spin polarization because in these low-dimensional systems the resulting increase in the effective  $d$  bandwidth took the  $d$  band beyond the magnetic saturation limit. In the case of pure Ni systems, spin polarization comes mainly from the few  $d$  holes in the minority part of the density-of-states; the majority part is nearly saturated. Since the number of holes is very small, the magnetic moment of Ni systems is generally much smaller than in other magnetic transition-metal systems, such as those composed of Fe. Figure 2 shows that in the presence of the delocalized  $sp$ -type states of Al, the majority part of the Ni density-of-states is no longer saturated, and magnetization consequently vanishes.

Before using the real-space TB model and parametrization described in the previous section to investigate whether or not the previously determined Ni cluster ground states have a magnetic moment, we first tested it by using it to recalculate the electronic structure in the Ni monolayer case and comparing the resulting LDOS with those obtained using the *ab initio* TB-LMTO method. The two methods were found to give qualitatively similar results as regards hybridization, bandwidths, etc., especially for the occupied states and those close to the Fermi level. In particular, no magnetization was obtained in the Ni monolayers using the exchange parameter that affords the correct magnetic moment of Ni in the bulk fcc structure ( $0.60\mu_B$ , where  $\mu_B$  is the Bohr magneton; Ref. 37). We accordingly proceeded to use the TB model parametrization to study Ni clusters.

Figure 3 shows the LDOS at some representative sites of

the ground-state system obtained for  $\text{Ni}_6$ . In this case there are two inequivalent Ni sites that have different LDOS because of their different local environments. The clusters were found to be nonmagnetic for the same reasons as the Ni monolayers:  $sp-d$  hybridization and the resulting increase in the effective  $d$  bandwidth, as reflected in the partial  $sp$  and  $d$  densities-of-states. The other  $\text{Ni}_n$  clusters ( $2 \leq n \leq 10$ ) behaved similarly.

#### IV. SUMMARY AND CONCLUSIONS

In this paper we used the VC EAM Ni-Al potential to compute the ground-state structures of small  $\text{Ni}_n$  clusters ( $2 \leq n \leq 10$ ) on or just below the Al (001) surface. Our results showed that embedded clusters are always more stable than the adsorbed clusters, a finding which clarifies and improves the simulation results reported in Ref. 11. The magnetic properties of the  $\text{Ni}_n/\text{Al}(001)$  systems were determined using a self-consistent TB method, the accuracy of which was previously tested by comparing the results it afforded for

monolayers supported on or embedded in Al(001) with those derived using the *ab initio* TB-LMTO method. It was found that, due to  $sp-d$  hybridization effects, both embedded or supported Ni monolayers, and embedded Ni clusters, are nonmagnetic.

Work is currently being undertaken to determine whether clusters of more magnetic transition-metal atoms, such as Fe and Co, can sustain magnetic moments when deposited on Al.

#### ACKNOWLEDGMENTS

We are grateful to J. Izquierdo for useful discussions, and to C. Rey for his help in computing. This work was supported by the DGICYT, Spain (Project PB98-0368-C02), the Junta de Castilla-León (Grant VA 70/99), and the Xunta de Galicia (Project PGIDT99PXI20604B). R. Robles acknowledges an FPI grant from the Spanish Ministry of Education and Culture.

- 
- <sup>1</sup>W. F. Smith, *Structure and Properties of Engineering Alloys* (McGraw-Hill, New York, 1981).
- <sup>2</sup>T. Sands, *Appl. Phys. Lett.* **52**, 197 (1988).
- <sup>3</sup>V. Shutthanandan, A. A. Saleh, and R. J. Smith, *J. Vac. Sci. Technol. A* **11**, 1780 (1993).
- <sup>4</sup>V. Shutthanandan, A. A. Saleh, A. W. Denier van der Gon, and R. J. Smith, *Phys. Rev. B* **48**, 18 292 (1993).
- <sup>5</sup>A. A. Saleh, V. Shutthanandan, and R. J. Smith, *Phys. Rev. B* **49**, 4908 (1994).
- <sup>6</sup>V. Shutthanandan, A. A. Saleh, N. R. Shivaparan, and R. J. Smith, *Surf. Sci.* **350**, 11 (1996).
- <sup>7</sup>N. R. Shivaparan, V. Krasemann, V. Shutthanandan, and R. J. Smith, *Surf. Sci.* **365**, 78 (1996).
- <sup>8</sup>N. R. Shivaparan, V. Shutthanandan, V. Krasemann, and R. J. Smith, *Surf. Sci.* **373**, 221 (1997).
- <sup>9</sup>A. A. Saleh, V. Shutthanandan, N. R. Shivaparan, R. J. Smith, T. Tran, and S. A. Chambers, *Phys. Rev. B* **56**, 9841 (1997).
- <sup>10</sup>A. F. Voter and S. P. Chen, in *Characterization of Defects in Materials*, edited by R. W. Siegel, J. R. Weertman, and R. Sinclair, MRS Symposia Proceedings No. 82 (Materials Research Society, Pittsburgh, 1987), p. 175.
- <sup>11</sup>R. C. Longo, O. Diéguez, C. Rey, and L. J. Gallego, *Eur. Phys. J. D* **9**, 543 (1999).
- <sup>12</sup>J. Izquierdo, A. Vega, and L. C. Balbás, *Phys. Rev. B* **55**, 445 (1997).
- <sup>13</sup>P. Ballone and R. O. Jones, *Chem. Phys. Lett.* **233**, 632 (1995).
- <sup>14</sup>S. Bouarab, A. Vega, M. J. López, M. P. Iñiguez, and J. A. Alonso, *Phys. Rev. B* **55**, 13 279 (1997).
- <sup>15</sup>S. E. Apsel, J. W. Emmert, J. Deng, and L. A. Bloomfield, *Phys. Rev. Lett.* **76**, 1441 (1996).
- <sup>16</sup>R. P. Gupta, *Phys. Rev. B* **23**, 6265 (1981).
- <sup>17</sup>P. R. Schwoebel, S. M. Foiles, C. L. Bisson, and G. L. Kellogg, *Phys. Rev. B* **40**, 10 639 (1989).
- <sup>18</sup>S. M. Foiles, M. I. Baskes, and M. S. Daw, *Phys. Rev. B* **33**, 7983 (1986).
- <sup>19</sup>M. C. Fallis, M. S. Daw, and C. Y. Fong, *Phys. Rev. B* **51**, 7817 (1995).
- <sup>20</sup>S. C. Wang and G. Ehrlich, *Surf. Sci.* **239**, 301 (1990).
- <sup>21</sup>C. Rey, J. García-Rodeja, and L. J. Gallego, *Phys. Rev. B* **54**, 2942 (1996).
- <sup>22</sup>M. Calleja, C. Rey, M. M. G. Alemany, L. J. Gallego, P. Ordejón, D. Sánchez-Portal, E. Artacho, and J. M. Soler, *Phys. Rev. B* **60**, 2020 (1999).
- <sup>23</sup>A. Vega, L. C. Balbás, H. Nait-Laziz, C. Demangeat, and H. Dreyssé, *Phys. Rev. B* **48**, 985 (1993).
- <sup>24</sup>O. K. Andersen and O. Jepsen, *Phys. Rev. Lett.* **53**, 2571 (1984).
- <sup>25</sup>O. K. Andersen, Z. Pawłowska, and O. Jepsen, *Phys. Rev. B* **34**, 5253 (1986).
- <sup>26</sup>W. H. Press, B. P. Flannery, S. A. Teukolsky, and W. T. Vetterling, *Numerical Recipes* (Cambridge University Press, Cambridge, 1988).
- <sup>27</sup>G. J. Ackland and R. Thetford, *Philos. Mag. A* **56**, 15 (1987).
- <sup>28</sup>A. Vega, J. Dorantes-Dávila, L. C. Balbás, and G. M. Pastor, *Phys. Rev. B* **47**, 4742 (1993).
- <sup>29</sup>D. A. Papaconstantopoulos, *Handbook of the Band Structure of Elemental Solids* (Plenum, New York, 1986).
- <sup>30</sup>V. Heine, *Phys. Rev.* **153**, 673 (1967).
- <sup>31</sup>U. von Barth and L. Hedin, *J. Phys. C* **5**, 1629 (1972).
- <sup>32</sup>P. Hohenberg and W. Kohn, *Phys. Rev.* **136**, B864 (1964).
- <sup>33</sup>W. Kohn and L. J. Sham, *Phys. Rev.* **140**, A1133 (1965).
- <sup>34</sup>R. Haydock, in *Solid State Physics*, edited by H. Ehrenreich, F. Seitz, and D. Turnbull (Academic, New York, 1980), Vol. 35, p. 215.
- <sup>35</sup>F. Patthey, C. Massobrio, and W.-D. Schneider, *Phys. Rev. B* **53**, 13 146 (1996).
- <sup>36</sup>W.-D. Schneider, H.-V. Roy, P. Fayet, F. Patthey, B. Delley, and C. Massobrio, in *Cluster Assembled Materials*, edited by K. Sattler, Materials Science Forum, Vol. 232 (Trans Tech Publications, Switzerland, 1996), p. 51.
- <sup>37</sup>N.W. Ashcroft and N.D. Mermin, *Solid State Physics* (Saunders College, Philadelphia, 1976).